Structural Evolution in Iodine-Doped Poly(3-alkylthiophenes)

M. J. Winokur* and Paula Wamsley

Department of Physics, University of Wisconsin, Madison, Wisconsin 53706

Jeff Moulton,† Paul Smith,† and A. J. Heeger‡

Departments of Materials Science and Physics, University of California, Santa Barbara, California 93106

Received November 30, 1990; Revised Manuscript Received January 23, 1991

ABSTRACT: Poly(3-alkylthiophenes) are found to undergo continuous structural transformations upon doping with iodine vapor. Doping is characterized by an initial increase and then a reduction in the interlayer repeat. This process involves cooperative motions of the alkyl chains, the polymeric backbones, and the dopant ions, whereby alkyl chain interdigitation is initially suppressed and then encouraged. Structure factor calculations identify the specific molecular motions by both polymer and dopant.

I. Introduction

Determination of conducting polymer structures, when either doped or undoped, is an important goal for developing a better understanding of these unusual materials. For crystalline hosts, diffraction methods are appropriate and an extensive literature exists for many of the unsubstituted compounds.[1-7] In these materials, dopant-ion uptake initiates a combination of translational and rotational motions by the polymeric main chains with the subsequent formation of various doped phases. Short-side-chain substitution at the 3-carbon position of polythiophene stabilizes a helical formation of the thiophene units in which the dopant is situated between adjacent arcs of the helix.[8] For the host materials so far studied, the onset of doping is primarily characterized by a simple two-phase coexistence.

There is considerably less structural information available for larger side-chain-substituted conducting polymers (Figure 1a). This process results in soluble compounds,[9] which can be studied while in solution,[10,11] as a constituent of Langmuir–Blodgett films,[12] or when cast. Nominally, this substitution restores backbone planarity and induces a lamellar configuration, isomorphic to nonelectroactive polymers,[13,14] whereby the alkyl chains act as spacers between two-dimensional sheets[15-17] formed by stacking the polymer main chains one above another (Figure 1b). Not only does this packing enhance the diffusion kinetics but it also serves to optimize conduction within individual stacks by allowing for π-electron orbital overlap between adjacent polymer chains. Furthermore, this chemical modification introduces new degrees of freedom that must be accommodated upon doping.

In this report we present initial in situ X-ray diffraction results from oriented iodine-doped poly(3-*n*-octylthiophene) (P3OT) and poly(3-*n*-dodecylthiophene) (P3DT) films, highlighting the general features of this doping process and the presence of striking structural behavior unavailable to unsubstituted systems. In contrast to the doping evolution of unsubstituted compounds, dopant uptake in P3OT is marked by continuous variations of structure within a "single" phase. We find that there is extreme sensitivity of the side-group orientations to the presence of the dopant ions. This conformational change, when combined with rotation of the polymeric backbone about its chain axis, results in dramatic variations in the intralayer and interlayer spacings within semicrystalline regions of the film. Two distinct doping regimes are observed. Initial doping is marked by a rapid increase in the interlayer repeat. Further doping yields a dramatic

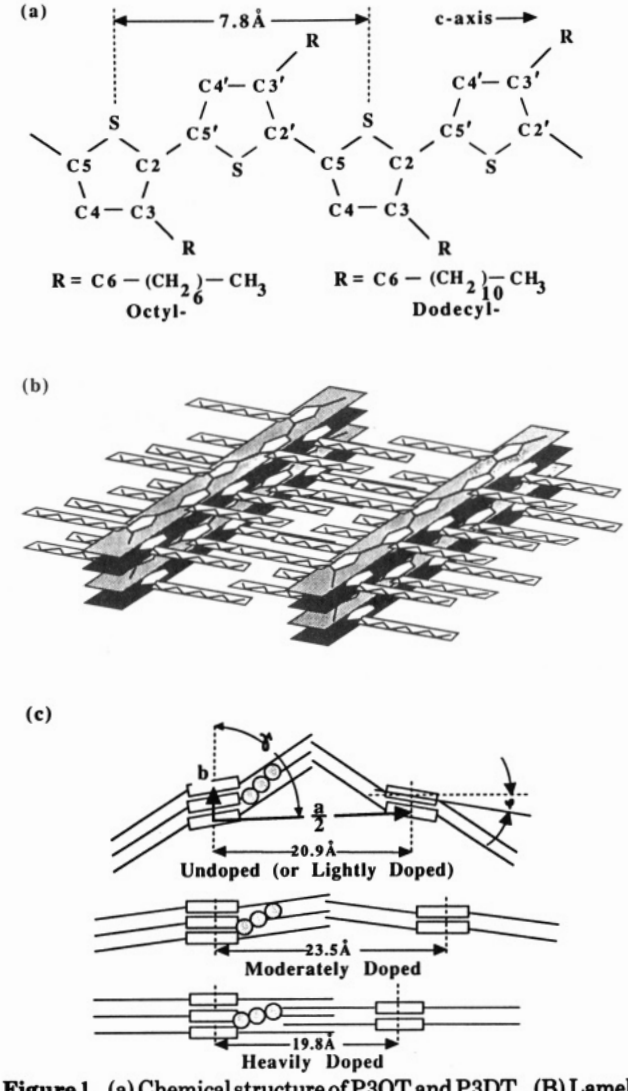

Figure 1. (a) Chemical structure of P3OT and P3DT. (B) Lamellar packing of the poly(3-alkylthiophenes). (c) Projected equatorial structure of P3OT at various doping levels. Note the changes in the iodine position (hatched circles).

† Department of Materials Science, University of California.
‡ Department of Physics, University of California.

0024-9297/91/2224-3812$02.50/0

reduction in this spacing. In fact, P3OT exhibits its smallest interlayer spacing near *saturation* doping (at ≈55 mol % of I_3^- referenced to the alkylthiophene monomer). This saturation structure also evidences a new equatorial periodicity. With use of structure factor (SF) calculations, the basic structure within undoped films and the molecular degrees of freedom necessary for the doping-induced transformation can be determined. These calculations also enable a partial determination of the dopant-ion location within the host matrix. From these results it is evident that the dopant lies to the side of the main-chain stacks and has only a slight influence on the average intralayer chain-to-chain spacing.

II. Experimental Section

The poly(3-alkylthiophene) samples utilized in this study were synthesized by Neste Oy (P3OT) and at Santa Barbara (P3DT) using a direct oxidative coupling of 3-octylthiophene and 3-dodecylthiophene, respectively, by $FeCl_3$.[18] After synthesis, the $FeCl_3$ was extracted, and the films were dissolved in chloroform. These solutions were then filtered and poured directly onto glass slides. After solvent evaporation, the films were lifted by methanol and clamped into a simple home-built stretching device. Uniaxially stretching ratios as high as 4:1 were achieved at drawing temperatures ca. 100 °C.

The X-ray diffraction facility consisted of an X-ray source, a computer-controlled diffractometer, and an array detector.[19] The X-ray source, a 15-kW Elliot GX-21 rotating anode generator, utilized a copper target ($\lambda_{K\alpha}$ = 1.541 Å) fitted with a Union Carbide bent-graphite monochromator. The cross-sectional area of the incident X-ray beam at the sample was adjusted to ≈2.0 × 2.0 mm². The position-sensitive array detector consisted of a refrigerated EG&G 1412XR silicon diode array and associated interface electronics. The detector's spatial resolution was set by forming 16 pixel groups from the detector's 960 accessible 25 μm × 2 mm pixels. This diode array was located ≈30 cm from the scattering center and subtended a 2θ angle of ≈4.5°. In order to minimize nonlinearities across the detector, a correction factor for each group was included and the 2θ step size for each individual data collection point was limited to 0.5°.

These studies were performed by using ≈40-μm-thick samples of the stretch-oriented solution-cast films. Dopant uptake produced substantial reductions in the transmitted intensities so that the dopant concentrations could be independently estimated by scanning the (111) reflection of fine nickel wire (Johnson-Matthey) mounted with the samples. For the in situ methodology, a home-built vapor-doping cell with thin (≈5 μm) mica windows was employed. Both the temperature of an iodine reservoir and that of the polymer could be adjusted independently. Poly(alkylthiophenes) are known to undergo thermally induced dopant desorption,[20,21] a process that partially aided the undoping cycle. Equatorial (*hk*0) scans, which probe the projected polymer structure in directions perpendicular to the polymer chain axis (or *c* axis), were acquired continuously throughout doping cycles.[22]

III. Results and Discussion

Figure 2 displays (*hk*0) profiles from the initial doping cycle of a P3OT sample. The most notable features are the intense reflection at small angles, the evenly spaced reflections at higher angles, and a broader "peak" near 23.4°. For the undoped film (scan a), the low-angle peaks correspond to first-order and various higher order reflections from the 20.9 Å interlayer spacing (referred to as (*h*00) reflections). The 23.4° peak is actually a superposition of closely spaced (*hk*0) reflections and roughly corresponds to the 3.83 Å intralayer spacing. These peaks sit atop a smoothly decaying background and two broad peaks centered at ≈5° and ≈20°. The low-angle peak is thought to arise from scattering by residual regions of nematic ordering and/or amorphous fractions while the broad

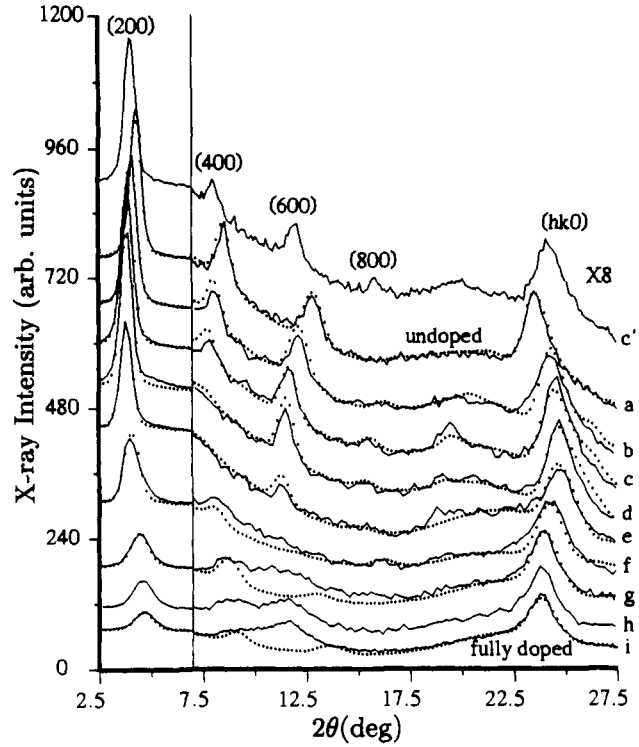

Figure 2. Equatorial profiles of the experimental (solid lines) data and calculated SF's (dotted lines; includes a background correction) during iodine doping of P3OT (from a to i). The scan labeled c' was acquired during an undoping cycle and has a dopant concentration close to that of scan c.

feature, at 20°, is indicative of appreciable hydrocarbon disorder originating from all portions of the film.[15]

Also seen in Figure 2 is the gradual evolution in the peak positions during dopant-ion uptake (a–i). The initial shift to smaller angle, or increased interlayer spacing (from a to e), is evident in all visible (*h*00) reflections. Furthermore, the (*h*00) radial peak widths are nearly constant throughout this portion of the doping process, suggesting the presence of relatively homogeneous doping. For P3OT, the maximum spacing is 23.5 Å (at 18% mol wt of I_3^-) and represents a 12% increase over that of the starting material. Conversely, the reverse process occurs in the (*hk*0) peak superposition and the intralayer repeat shrinks to 3.65 Å. At higher dopant levels the reduction in interlayer spacing is indicated by the shift of all (*h*00) reflections to higher angles (e–i). At saturation the interlayer repeat is 19.8 Å, a 16% drop from its maximum and 1.1 Å less than that at the start. During this latter process the intralayer repeat increases slightly to 3.77 Å. In contrast to the initial doping regime, modest broadening of the (*h*00) radial peak widths is detected.

As the inset of Figure 3 shows, both P3OT and P3DT exhibit analogous behavior. For P3DT, the initial interlayer increase is from 25.9 Å to a maximum of 31.2 Å at ≈25% mol wt of I_3^-. Further doping induces a contraction to a final value of 28.7 Å at an I_3^- concentration of ≈50% mol wt. For P3DT the net increase is 5.3 Å (compared to 2.6 Å for P3OT with its smaller alkyl chain) whereas the overall contraction at the higher dopant concentrations is substantially less.

Undoping involves a reverse process with expansion and then slight contraction of the interlayer spacing. Surprisingly, expansion apparently occurs only after a significant fraction of iodine has desorbed from the sample. Complete reversibility is difficult to establish due to the

Table I
Structural Data for P3OT

interlayer spacing, Å	intralayer spacing, Å	mean area per chain, Å²	I_3^- conc, mol wt %: X-ray absorpn	I_3^- conc, mol wt %: structure factor
20.9	3.83	80.2	0	0
21.9	3.71	81.1	2	4
22.8	3.68	84.0	4	6
23.1	3.65	84.3	6	11
23.5	3.68	88.6	18	19
21.9	3.69	80.9	34	24
20.9	3.75	77.3	50	26
19.8	3.77	74.8	55	38

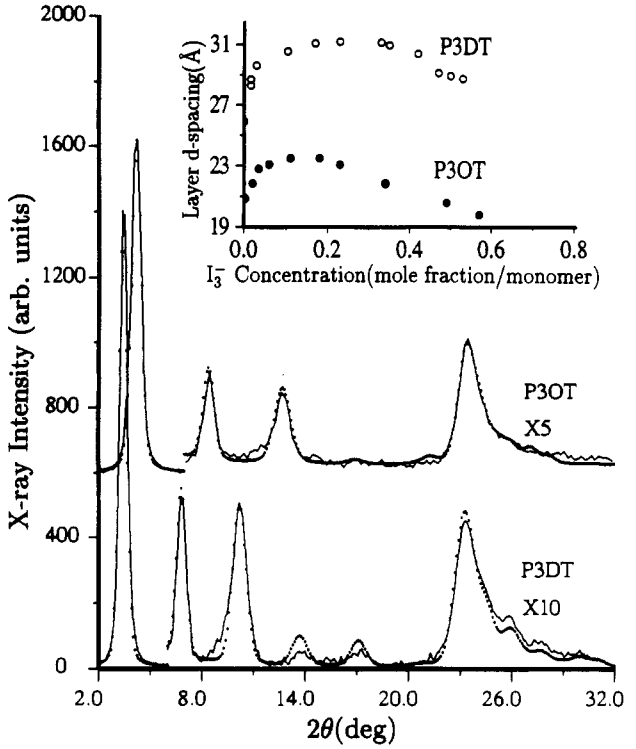

Figure 3. Comparison of the experimental equatorial data (solid lines) and calculated profiles (dotted lines) for undoped P3OT and P3DT using the model in Figure 1c, top. The background (as described in the text) has been subtracted from the experimental profiles. Inset: Interlayer spacing as a function of dopant concentration (as determined by X-ray absorption) for P3OT and P3DT during the initial doping cycle.

residual iodine and thermal heating of the sample. A qualitative comparison of two P3OT scans (c and c′ in Figure 2) from doping and undoping cycles at nearly equal dopant concentrations shows the strong structural similarity (indicated by a comparison of the relative peak intensities).

To address the microscopic reorganizations necessary, SF calculations were performed. Though there is insufficient information to determine individual atomic positions, the constraints enforced by chemical bonding and conformational energetics restrict the preferred main-chain and side-group configurations. Similar techniques have been used successfully in the analysis of lamellar phases in various neat soaps.[23] In our study, the backbones were restricted to a trans-planar zigzag conformation with an invariant 7.8 Å c axis repeat.[4] This structure creates significant gaps between adjacent alkyl chains along each side of the backbone. The alkyl chains were also required to maintain an all-trans conformation with conventional bond lengths and bond angles. The only adjustable polymeric parameters were the projected equatorial lattice constants (see Figure 1c, top), rotation of the entire polymer about its chain axis (i.e., setting angle ϕ), rotation of the entire alkyl chain about the C3–C6 bond (a dihedral or torsional angle), and variations in the C2–C3–C6 bond angle. This latter degree of freedom primarily influenced nonequatorial profiles.[24]

For undoped P3OT and P3DT, the SF calculations are incompatible with interdigitation of side chains by either neighboring intralayer or interlayer alkyl chains. While a broad continuum of rotations about the chain axis combined with adjustment to the previously defined dihedral angle reproduce the intensity variations of the (h00) reflections, values of 5° and 75° for P3OT and 15° and 65° for P3DT work well for all of the scattering data.[24] This motion twists the alkyl chains out of the plane formed by the trans-planar thiophene backbone and develops a more compact nesting of the alkyl chains within the stacked layers. It also generates an effective ≈40° alkyl chain tilt away from the layer perpendicular (seen in Figure 1c, top), and this resultant packing hinders interlayer overlap. Excellent fits (shown in Figure 3) are obtained with projected (nonprimitive) 2D unit cells of a = 42.0 Å, b = 7.67 Å, and γ = 87° and a = 51.9 Å, b = 7.74 Å, and γ = 86° for P3OT and P3DT, respectively. Specifically, the intensity variations in the high-angle wings of the superposition (hk0) "peak" are well reproduced.

This specific model employs a unit cell consisting of four polymer chains with two monomer units per chain. Thus we obtain an alternation of the rotational degrees of freedom from one layer to the next and a $c/2$ staggering of the polymer chains immediately adjacent (above and below) within individual sheets. A more comprehensive model would encompass disorder effects such as local distortions by the alkyl chains to accommodate the dopant ions or inaccuracies in the side-chain head-to-tail coupling (of ≈20%).[17]

To assess the iodine contribution, additional parameters were introduced. Iodine doping involves a disproportionation reaction to form various linear polyiodides and, at light dopant levels, I_3^- is thought to dominate.[25] In addition, the minimal changes in the intralayer spacing locate the dopant along side the main chains. For these reasons, the SF calculations include fractional I_3^- contributions from ions that occupy any position while squeezed between two adjacent alkyl chains on one side of the polymer strand and bounded by two additional alkyl chains from above and below.

As iodine doping proceeds, the peak position shifts are accompanied by subtle changes in the relative peak intensities, and this indicates reorganizations within the unit cell itself. For P3OT, the following sequence is observed: the (400) reflection decreases rapidly until unobservable and then gradually reappears, the (600) reflection initially increases slightly and then decreases until unobservable, and higher order (h00) peaks appear only briefly in scans c and d of Figure 2. There are also substantial changes in the (hk0) peak superposition profile, particularly on the high-angle side. As the calculated equatorial profiles show (dotted lines in Figure 2), this progression can be accurately reproduced by introducing a gradual rotation of the dihedral angle and of the chain axis rotation toward final values of approximately zero degrees combined with a smoothly increasing iodine contribution.

At very light doping levels the SF calculations are insensitive to the polyiodide contribution; hence, the initial (h00) intensity variations result primarily from polymer host motions. Near dopant concentrations of 5% mol wt I_3^-, the concentration can be fixed and the location of I_3^-

ions discerned. The iodine atom closest to the main chain is ≈3 Å from the sulfur atom, and the dopant-ion long axis must be tilted 65° from the layer perpendicular (see Figure 1c, top). This orientation allows the iodine atoms to locate within a "cage" formed by the four surrounding alkyl chains. While the (*h*00) intensity variations are well-matched, the (*hk*0) superposition fit is only qualitatively correct, for the calculated profiles develop a more pronounced high-angle wing than is experimentally observed. When the 2D lattice parameters from these structure factor calculations are used, the mean area per alkyl chain can be determined at selected points during the doping process, and these values are summarized in Table I for P3OT.

Dopant uptake also involves lowering of the iodide tilt to accommodate changes in the cage dimensions as the dihedral angle is reduced. At the maximum P3OT interlayer spacing, our calculations suggest a ≈30° dihedral angle, chain rotation to ≈0°, and an iodide tilt of 45°. By now the effective alkyl chain tilt is sufficiently reduced so that further doping results in interdigitation of alkyl chains from neighboring layers (shown in Figure 1c, middle). As the overlap increases there is a corresponding reduction in the interlayer spacing. This process is consistent with a continued lessening in the dihedral angle, but the SF sensitivity to this parameter is lessened by the growing iodine contribution. We also find readjustments in the iodide tilt angles toward a final value of ≈30°. This motion is accompanied by a translation of the dopant toward the polymer chain axis and along the *b* axis direction so that the end of the ion appears to bridge two polymer chains (see Figure 1c, bottom).

At heavier I_3^- concentrations, these calculations are complicated by the appearance of a new scattering feature near 11.8° (see Figure 2, i), or, equivalently, at a *d* spacing of 7.5 Å. This feature also evolves smoothly by initially appearing as a broad ill-defined "peak" in scan f and then increasing in intensity and narrowing somewhat in width as the sample approaches saturation. While the precise origin of this new periodicity is not fully understood, this feature probably represents an additional ordering (at twice the intralayer spacing) by the dopant ions. Nominally, there is a single dopant-ion site per alkylthiophene monomer and each alkyl side chain is shared equally among four of these suggestive cages. Hence, at the highest dopant levels there is a strong likelihood that an I_3^- ion in its respective site will directly influence the occupancy at neighboring sites. This would then induce a further ordering of the dopant ions themselves. A partial account of this ordering process can be approximated by introducing a simplistic weighting of the iodine distribution, but an accurate picture requires a more sophisticated model. If this scattering is neglected, the calculated profile suggests a saturation concentration of 38 mol % of I_3^-, a value close to the ≈55% obtained from absorption measurements.

IV. Conclusion

These results identify and characterize the unusual reorganizations that can occur in the doped phases of alkyl-substituted conducting polymers. For iodine-doped samples, this substitution allows for dramatic and apparently continuous structural evolution in which there is a crossover from a packing configuration that strongly suppresses alkyl interdigitation into one in which interdigitation is quite pronounced. Among the various p-type dopants, iodine is often selected for its chemical simplicity and its straightforward doping procedures. In this example, iodine forms a small linear ion, which can locate within a cage formed by four surrounding alkyl chains. Since this is, to our knowledge, the first detailed report of dopant-induced structural evolution in these alkyl-substituted conduction polymers, generalization to other substituted hosts or to different dopants must also be addressed. Dopants of substantially different sizes may yield fundamentally different structural reorganizations. Even for nominally identical host polymers, variations in the intrinsic polymer characteristics (e.g., degree of polymerization, cross-linking) could influence the physical behavior ultimately expressed.

Acknowledgment. This work was supported by the University of Wisconsin (P.W.), by the NSF DMR Grant No. DMR-8917530 (M.J.W.), and jointly by DARPA–AFOSR and monitored by AFOSR under Contract No. F49620-88-C-0138 (J.M., P.S., and A.J.H.).

References and Notes

(1) Fincher, C. R.; Chen, C. E.; Heeger, A. J.; MacDiarmid, A. G.; Hastings, J. B. *Phys. Rev. Lett.* **1982**, *48*, 100.
(2) Jozefowicz, M. E.; Laversanne, R.; Javadi, H. H. S.; Epstein, A. J.; Pouget, J. P.; Tang, X.; MacDiarmid, A. G. *Phys. Rev. B* **1989**, *39*, 12958.
(3) Granier, T.; Thomas, E. L.; Gagnon, D. R.; Lenz, R. W., Jr.; Karasz, F. E. *J. Polym. Sci. Phys.* **1989**, *24*, 2793.
(4) Brüchner, S.; Porzio, W. *Makromol. Chem.* **1989**, *89*, 961.
(5) Baughman, R. H.; Murthy, N. S.; Miller, G. G.; Shacklette, L. W. *J. Chem. Phys.* **1983**, *79*, 1065.
(6) Baughman, R. H.; Murthy, N. S.; Miller, G. G. *J. Chem. Phys.* **1983**, *79*, 515.
(7) Wieners, G.; Weizenhofer, R.; Monkenbusch, M.; Stamm, M.; Lieser, G.; Enkelmann, V.; Wegner, G. *Makromol. Chem., Rapid Commun.* **1985**, *6*, 425.
(8) Garnier, F.; Tourillon, G.; Barraud, J. Y.; Dexpert, H. *J. Mater. Sci.* **1985**, *20*, 2687.
(9) Jen, K. Y.; Oboodi, R.; Elsenbaumer, R. L. *Polym. Mater. Sci. Eng.* **1985**, *53*, 79.
(10) Rughooputh, S. D. D. V.; Hotta, S.; Hegger, A. J.; Wudl, F. *J. Polym. Sci., Polym. Phys.* **1987**, *25*, 1071.
(11) Aime, J. P.; Bargain, F.; Schott, M.; Eckhardt, H.; Miller, G. G.; Elsenbaumer, R. L. *Phys. Rev. Lett.* **1987**, *62*, 55.
(12) Watanabe, I.; Cheung, J. H.; Rubner, M. *J. Chem. Phys.*, in press.
(13) Ballauff, M.; Rosenau-Eichin, R.; Fischer, E. W. *Mol. Cryst. Liq. Cryst.* **1988**, *155*, 211.
(14) Ballauff, M.; Berger, K. *Mol. Cryst. Liq. Cryst.* **1988**, *157*, 109.
(15) Winokur, M. J.; Spiegel, D.; Kim, Y. H.; Hotta, S.; Heeger, A. J. *Synth. Met.* **1989**, *28*, C419.
(16) Gustafsson, G.; Inganäs, O.; Osterholm, H.; Laakso, J., to be published.
(17) Leclerc, M.; Diaz, F. M.; Wegner, G. *Makromol. Chem.* **1989**, *190*, 3105.
(18) Inganäs, O.; Salaneck, W. R.; Osterholm, H.; Laaksa, J. *Synth. Met.* **1988**, *22*, 395.
(19) Chen, D.; Winokur, M. J.; Masse, M.; Karasz, F. E. *Phys. Rev. B* **1990**, *41*, 6759.
(20) Gustafsson, G.; Inganäs, O.; Nilsson, J. O.; Liedberg, B. *Synth. Met.* **1988**, *26*, 297.
(21) Nilsson, J. O.; Inganäs, O. *Synth. Met.* **1989**, *31*, 359.
(22) Cycling times for this experiment were typically a few weeks, but they can be accomplished in much less time.
(23) Skoulios, A. *Adv. Colliod Interface Sci.* **1967**, *1*, 79.
(24) Wamsley, P.; Winokur, M. J.; Moulton, J.; Smith, P.; Heeger, A. J., to be published.
(25) Matsuyama, T.; Sakai, H.; Yamaoka, H.; Maeda, Y.; Shirakawa, H. *J. Phys. Soc. Jpn.* **1983**, *52*, 2238.

Registry No. P3OT, 104934-51-2; P3DT, 104934-53-4; I_2, 7553-56-2.